ELSEVIER

Journal of Organometallic Chemistry 519 (1996) 185–194

Journal of Organometallic Chemistry

The synthesis and complexation of a ferrocene-based redox-active cryptand containing the phenanthroline unit

C. Dennis Hall *, Thi-Kim-Uyen Truong

Department of Chemistry, King's College London, Strand, London WC2R 2LS, UK

Received 1 December 1995

Abstract

The synthesis and characterisation of a ferrocene-based redox-active cryptand (**5**) containing a phenanthroline unit is described. Complex formation with a wide range of mono-, di- and trivalent cations was studied by $^{1}H/^{13}C$ nmr and uv–vis spectroscopy and the effects of complexation on the redox properties of (**5**) were monitored by cyclic voltammetry.

Keywords: Iron; Ferrocene; Cryptand; Phenanthroline; Redox activity; Macrocycle

1. Introduction

The synthesis, structure, electrochemistry and complex formation of cryptands containing metallocene units have attracted considerable attention in recent years [1–6]. These redox-active compounds are potentially useful as sensors for the detection and quantitative estimation of metal cations by electrochemical techniques [7], as catalysts in a variety of reactions [8], and as models for electron transfer in biological systems [9]. Some years ago, it was shown by Lehn and co-workers that irradiation of lanthanide complexes of certain cryptands (e.g. **1**) with ultraviolet light led to a red fluorescence at 610 nm due to energy transfer from the excited state of the bipyridyl units of (**1**) to the guest cation (Eu^{3+} or Tb^{3+}) followed by fluorescence from the $^{5}D_0$ and $^{5}D_4$ levels of complexed cations [10]. Application of this principle to redox-active cryptands enabled us to show that the cryptand (**2**) also formed a complex with Eu^{3+} which fluoresced at 620 nm on irradiation with ultraviolet light [11]. Since we have established that electrochemical oxidation of the metallocene unit within redox-active cryptates tends to expel highly charged cations from the cavity [12a,b], it was proposed that such a system might form the basis of a photochemical switch — in effect a voltage-regulated optical sensor. Since (**2**) is particularly difficult to prepare, it was decided to synthesise a redox-active cryptand containing the more readily derivatised phenanthroline unit as the 'photo antenna' for the system.

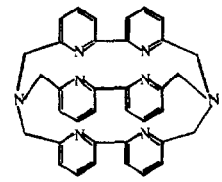

(1)

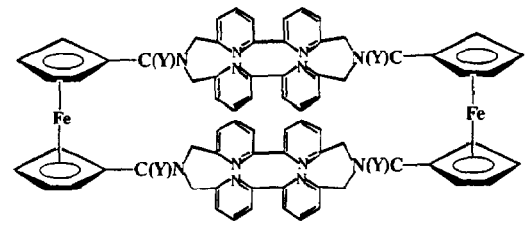

(2)

2. Results and discussion

The tetraazadioxa macrocycle (**3**) was synthesised by a literature procedure [12] and condensed with ferrocene

* Corresponding author.

PII S0022-328X(96)06172-4

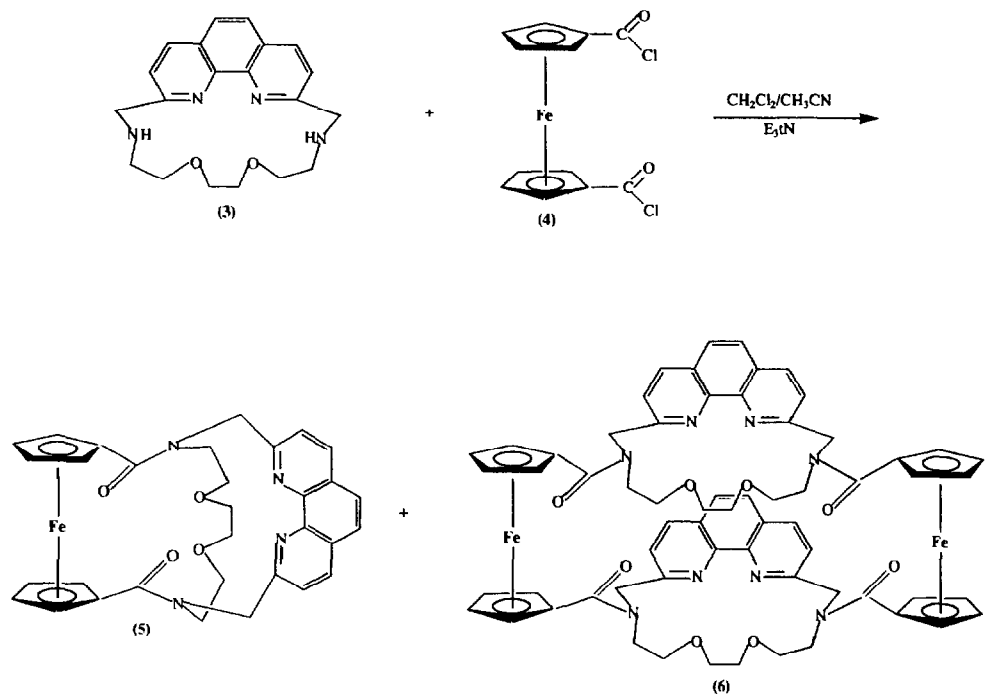

bis-acid chloride (**4**) to give a 24% yield (after chromatography) of the cryptand (**5**) with no evidence for the simultaneous formation of the dimer (**6**). A FAB mass spectrum gave an M + 1 peak at 591 to establish the momomeric structure and an accurate FAB mass spectrum ($M + Na^+ = 613.1510$) confirmed the molecular formula as $C_{32}H_{30}N_4O_4Fe$. The trans disposition of the carbonyl groups was confirmed, as in previous work [13], by the highly unsymmetrical nature of the ^1H data (Table 1(a)) which showed eight separate ferrocene hydrogen signals, six separate signals for the phenanthroline hydrogens (Fig. 1(a)) and a series of AB quartets for the remaining CH_2 signals. In addition, the ^{13}C spectrum (Table 1(b)) showed two carbonyl signals, eight ferrocene CH signals, six phenanthroline CH signals, four OCH_2 signals and four NCH_2 signals, as well as the *ipso*-carbons of the phenanthroline ring.

2.1. NMR studies of complex formation

Complexation of cryptand (**5**) with a variety of metal cations was then studied by ^1H and ^{13}C NMR and a typical example is reported in detail using calcium trifluoro-methane sulphonate as the guest species. (The trifluoro-methane sulphonate salts were used since they may be dried under vacuum at high temperature without the risk of explosion.) The ^1H NMR spectra of the phenanthroline region of 1 : 1 and 2 : 1 (host : guest) mixtures of (**5**) at 0.04 M and Ca $(CF_3SO_3)_2$ in $CDCl_3$ are shown in Fig. 1. In both cases the parent cryptand

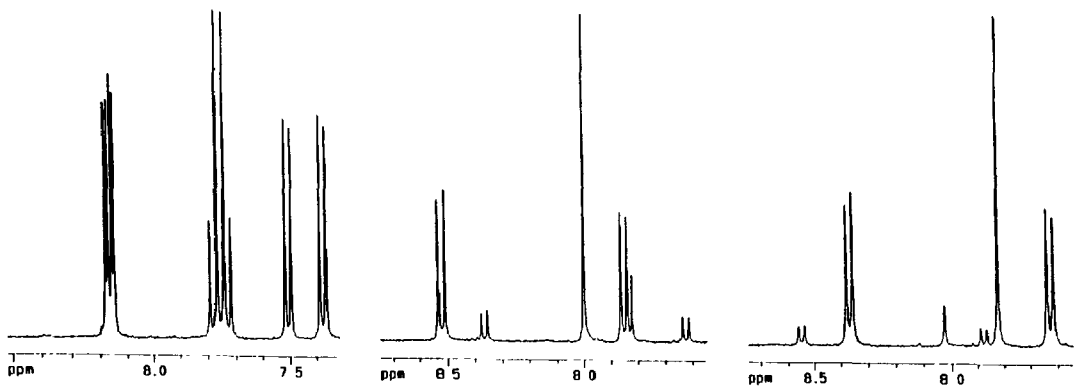

Fig. 1. NMR spectra in $CDCl_3$–CD_3CN of (a) the free ligand (**5**); (b) (**5**) + 1 molar equivalent $Ca(CF_3SO_3)_2$; (c) (**5**) + 0.5 molar equivalent $Ca(CF_3SO_3)_2$.

Table 1(a)
^{1}H NMR data of cryptand (5) in $CDCl_3$

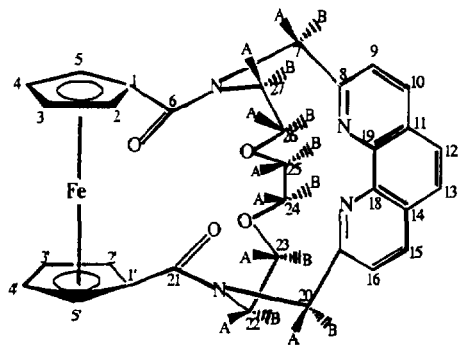

Atom	δ (^{1}H) (ppm)	Atom	δ (^{1}H) (ppm)	Atom	δ (^{1}H) (ppm)
H_2	4.95	H_{20A}	4.22	H_{27A}	4.76
H_3	4.45	H_{20B}	5.51	H_{27B}	3.62
H_4	4.76	H_9/H_{16}	7.38	H_{23A}	3.18
H_5	4.86	H_{10}/H_{15}	8.17	H_{23B}	2.81
$H_{2'}$	6.24	H_{12}/H_{13}	7.75	H_{26A}	3.65
$H_{3'}$	4.28	H_{13}/H_{12}	7.73	H_{26B}	3.28
$H_{4'}$	4.32	H_{15}/H_{10}	8.15	H_{24A}	3.67
$H_{5'}$	4.64	H_{16}/H_9	7.52	H_{24B}	2.95
H_{7A}	6.11	H_{22A}	5.19	H_{25A}	4.25
H_{7B}	4.33	H_{22B}	2.78	H_{25B}	3.97

(Fig. 1(a)) has been replaced by two new species (Figs. 1(b) and 1(c)) each exhibiting a pair of doublets and a singlet with the signals of both new species shifted considerably downfield relative to the host cryptand. Similar results were obtained with the other cations and the evidence suggests that the phenanthroline N atoms are involved in complex formation with the cations. The lower set of signals is due to a 1 : 1 complex and the higher field set (of higher intensity in Fig. 1(c)) is due to a 2 : 1 (host : guest) complex. Both complexes clearly contain a plane of symmetry which is consistent with the carbonyl groups becoming cis on complexation, as found previously [13]; this is confirmed by simplification of the remainder of the ^{1}H NMR and the ^{13}C NMR spectra (Tables 2(a) and (b)). Coordination of the amide carbonyls with Ca^{2+} was confirmed by shifts in the ^{13}C spectra of the C=O group (Table 2(a) and (b)) and by a shift of the amide carbonyl stretching vibration from 1621 cm^{-1} in the host to 1601 cm^{-1} in the 1 : 1 complex [14].

The effect of temperature on the ^{1}H NMR spectrum of the 1 : 1 mixture was also studied and, over a temperature range from 295 to 333 K, the ratio of 1 : 1/2 : 1 complex changed (reversibly) from 70% 1 : 1 to 78%

Table 1(b)
^{13}C NMR data of cryptand (5) in $CDCl_3$

Atom	δ(^{13}C) (ppm)	Atom	δ(^{13}C) (ppm)	Atom	δ(^{13}C) (ppm)
$C_1/C_{1'}$	85.2	C_7	55.0	C_{18}/C_{19}	146.6 ipso
C_2	74.3	C_8/C_{17}	158.1 ipso	C_{19}/C_{18}	145.8 ipso
C_3	70.9	C_9/C_{16}	121.3	C_{20}	58.2
C_4	72.7	C_{10}/C_{15}	136.5	C_{21}/C_6	170.6
C_5	73.8	C_{11}/C_{14}	128.0 ipso	C_{22}	47.5
$C_{1'}/C_1$	85.2	C_{12}/C_{13}	126.6	C_{23}	69.1
$C_{2'}$	71.5	C_{13}/C_{12}	125.4	C_{24}	71.7
$C_{3'}$	70.1	C_{14}/C_{11}	128.0 ipso	C_{25}	71.9
$C_{4'}$	70.2	C_{15}/C_{10}	136.0	C_{26}	70.5
$C_{5'}$	72.0	C_{16}/C_9	121.0	C_{27}	52.3
C_6/C_{21}	171.9	C_{17}/C_8	157.0 ipso		

Table 2(a)
^1H and ^{13}C NMR data for the 1:1 complex between (5) and Ca^{2+}

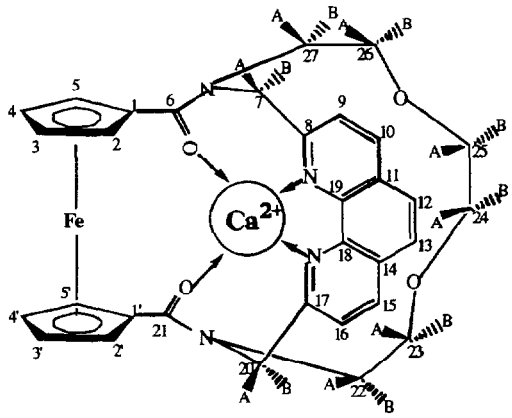

Atom	δ(^{1}H) (ppm)	Atom	δ(^{1}H) (ppm)
$H_2 \equiv H_{2'}$	5.11		
$H_3 \equiv H_{3'}$	4.49		
$H_4 \equiv H_{4'}$	4.46		
$H_5 \equiv H_{5'}$	5.16		
$H_{7A} \equiv H_{20A}$	5.90	$H_{7B} \equiv H_{20B}$	4.29
$H_9 \equiv H_{16}$	7.85		
$H_{10} \equiv H_5$	8.52		
$H_{12} \equiv H_{13}$	8.00		
$H_{22A} \equiv H_{27A}$	4 36	$H_{22B} \equiv H_{27B}$	3.33
$H_{23A} \equiv H_{26A}$	3 19	$H_{23B} \equiv H_{26B}$	2.53
$H_{24A} \equiv H_{25A}$	2.70	$H_{24B} \equiv H_{25B}$	2.70
$C_1 \equiv C_{1'}$	80.9	$C_9 \equiv C_{16}$	124.5
$C_2 \equiv C_{2'}$	75.2	$C_{10} \equiv C_{15}$	139.7
$C_3 \equiv C_{3'}$	70.3	$C_{11} \equiv C_{14}$	128.8
$C_4 \equiv C_{4'}$	71.4	$C_8 \equiv C_{13}$	127.0
$C_5 \equiv C_{5'}$	72.6	$C_{18} \equiv C_{15}$	144.3
$C_6 \equiv C_{21}$	175.7	$C_{22} \equiv C_{27}$	52.0
$C_7 \equiv C_{20}$	54.4	$C_{23} \equiv C_{26}$	66.9
$C_8 \equiv C_{17}$	160.2	$C_{24} \equiv C_{25}$	69.1

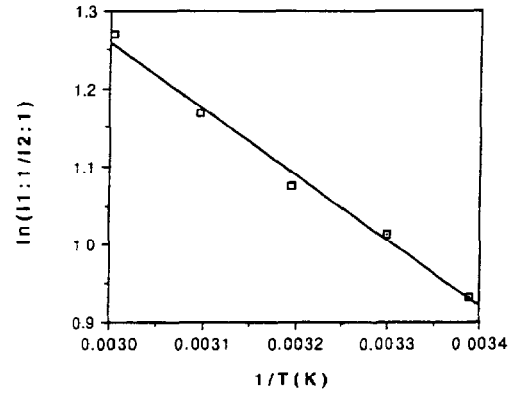

Fig. 2. Plot of ln(1:1 complex/2:1 complex) of (5) with $Ca(CF_3SO_3)_2$ vs. $1/T$ (K).

1:1, indicating that the 2:1 complex is in exothermic equilibrium with the 1:1 complex (Eq. (1)) with a ΔH° value of -7 kJ mol^{-1} (Fig. 2).

1:1 complex + (5) $\rightleftharpoons$ 2:1 complex (1)

2.2. Complex formation by uv–vis spectroscopy

Uv–vis spectroscopy was used to determine the stoichiometry of complexes formed by (5) at 1×10^{-3} M in $CDCl_3$–CD_3CN. The absorbance at constant wavelength (usually, $\lambda = 450$ nm) was monitored while adding one-tenth molar aliquots of 12 cationic triflates (Ag^+, K^+, Na^+, Mg^{2+}, Ca^{2+}, Sr^{2+}, Ba^{2+}, Y^{3+}, Eu^{3+}, Tb^{3+}, Dy^{3+} and Yb^{3+}) until no further change in absorbance was observed. A bathochromic shift of the d–d transition of the ferrocene unit (at 450 nm) was observed for each cation except K^+, with the magnitude

Table 2(b)
^1H and ^{13}C NMR data for the 2:1 complex between (5) and Ca^{2+}

Atom	δ ^{1}H (ppm)	Atom	δ ^{1}H (ppm)
$H_2 \equiv H_{2'}$	4.55		
$H_3 \equiv H_{3'}$	4.34		
$H_4 \equiv H_{4'}$	4.36		
$H_5 \equiv H_{5'}$	4.96		
$H_{7A} \equiv H_{20A}$	5.08	$H_{7B} \equiv H_{20B}$	3.84
$H_9 \equiv H_{16}$	7.63		
$H_{10} \equiv H_{15}$	8.37		
$H_{12} \equiv H_{13}$	7.82		
$H_{22A} \equiv H_{27A}$	4.15	$H_{22B} \equiv H_{27B}$	3.14
$H_{23A} \equiv H_{26A}$	3.08	$H_{23B} \equiv H_{26B}$	2.26
$H_{24A} \equiv H_{25A}$	2.62	$H_{24B} \equiv H_{25B}$	1.43
$C_1 \equiv C_{1'}$	80.8	$C_9 \equiv C_{16}$	124.1
$C_2 \equiv C_{2'}$	75.0	$C_{10} \equiv C_{15}$	139.4
$C_3 \equiv C_{3'}$	70.1	$C_{11} \equiv C_{14}$	128.0
$C_4 \equiv C_{4'}$	71.1	$C_{12} \equiv C_{13}$	126.9
$C_5 \equiv C_{5'}$	71.3	$C_{18} \equiv C_{19}$	145.6
$C_6 \equiv C_{21}$	174.4	$C_{22} \equiv C_{27}$	51.6
$C_7 \equiv C_{20}$	54.7	$C_{23} \equiv C_{26}$	67.3
$C_8 \equiv C_{17}$	160.9	$C_{24} \equiv C_{25}$	69.4

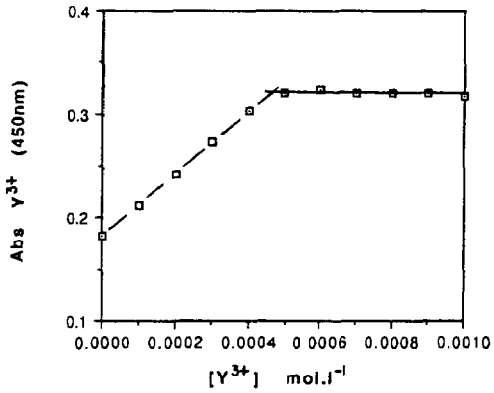

Fig. 3. Absorbance at $\lambda = 450$ nm for (5) vs. increasing $[Y^{3+}]$.

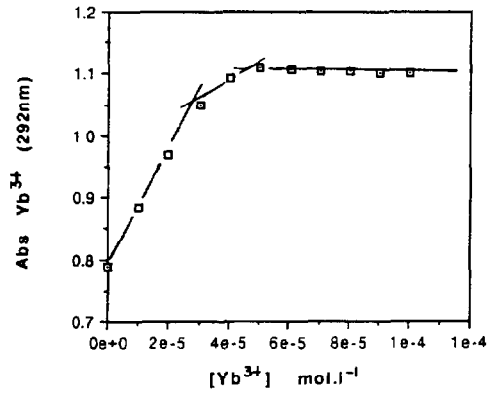

Fig. 5. Absorbance at $\lambda = 292$ nm for (5) vs. increasing $[Yb^{3+}]$.

of the shift and the intensity of the band dependent upon the size and charge of the cation used.

Plots of absorbance (at $\lambda = 450$ or 292 nm) vs. $[M^{n+}]$ were then created and found to fall into three categories. In the first, containing Y^{3+}, Eu^{3+}, Sr^{2+} and Ba^{2+} and as illustrated for Y^{3+} in Fig. 3, the ligand: M^{n+} stoichiometry was found to be 2:1. With Na^+, Mg^{2+} and Ca^{2+}, a mixture of 2:1 and 1:1 (host: guest) complexation was detected (Fig. 4), thus confirming the NMR results reported above for Ca^{2+}. Complexation with Yb^{3+} (Fig. 5), Dy^{3+} and Tb^{3+} showed a stoichiometry of 3:1 (host: guest) with a hint of a 2:1 stoichiometry appearing at higher metal ion concentrations. Finally, with Ag^+ the only observable stoichiometry was 1:1 (Fig. 6). With all these cations, however, the essentially linear response to the addition of each aliquot of cations suggests that the equilibrium constants for complexation are quite high. If one assumes a minimum of 90% complexation, then for a 1:1 stoichiometry (as with Ag^+) at 10^{-3} M in (5) K must be in the region of 10000, and for a 2:1 complex at the same level of complex formation the K value would be ca. 1.5×10^7. Thus, one might reasonably expect to see separate cyclic voltammogram (cv) waves with varying anodic shifts on complexation of each of the cations.

2.3. Cyclic voltammetry studies

The d-electrons of the ferrocene unit incorporated within the cryptate structures may or may not serve as donors for the bound cations, but when the iron atom of the host molecule is oxidised an electrostatic repulsion is created between the ferricinium ion of the host and the guest cation. This chemical change diminishes the binding capacity of the cryptand for cations which offers the possibility of creating a redox sensor and/or a cation switch.

Complexation of (5) with 11 cations (as for the uv studies but excluding K^+) was investigated by cyclic voltammetry. The experiments were carried out with propylene carbonate as solvent with (5) at 1.5 mM and with tetra-*n*-butylammonium perchlorate (TBAP) as supporting electrolyte. An electrode consisting of a Pt wire in a solution of ferrocene (0.01 M) and TBAP (0.1 M) in propylene carbonate was used as the reference. The cv of a 1.5 mM solution of (5) was recorded at ambient temperature and substoichiometric aliquots of metal cations were introduced sequentially to the ligand solution before each cv was recorded. Several categories of behaviour were again observed according to the cation used.

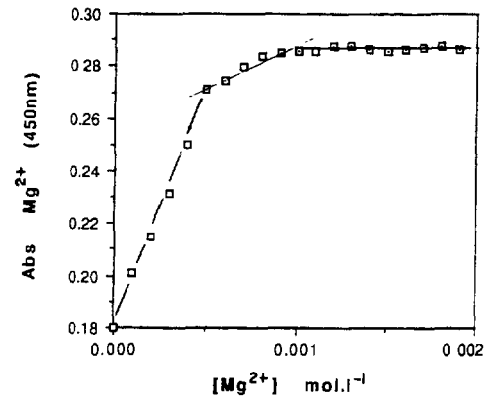

Fig. 4. Absorbance at $\lambda = 450$ nm for (5) vs. increasing $[Mg^{2+}]$.

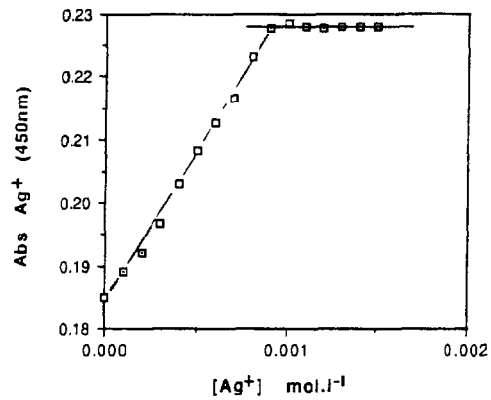

Fig. 6. Absorbance at $\lambda = 450$ nm for (5) vs. increasing $[Ag^+]$.

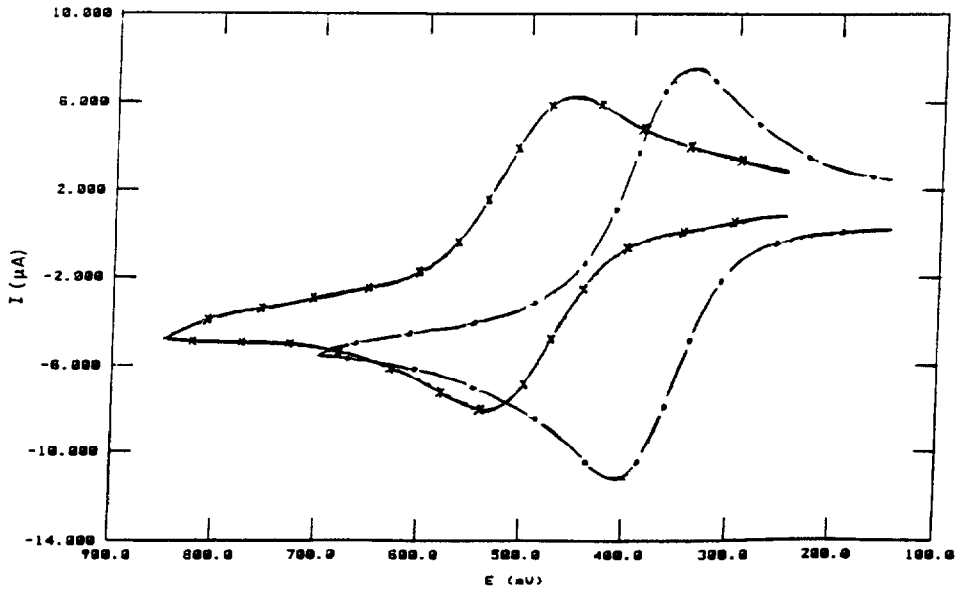

Fig. 7. Cyclic voltammograms for (5) complexing with Sr^{2+}: (– · – · –) free ligand; (– × – × –) 2(5) + Sr^{2+}.

With Y^{3+}, Eu^{3+}, Sr^{2+} and Ba^{2+}, addition of half an equivalent of cation gave a single electrochemical wave with, in each case, an anodic shift relative to the parent cryptand (Fig. 7). Addition of further aliquots of the cations failed to change the potential of the new cv wave and it was concluded that the stoichiometry of each of these complexes was 2:1 (host:guest) which confirms the results from the uv–vis experiments.

Addition of half an equivalent of Na^+ or Ca^{2+} also produced a single anodically shifted cv wave corresponding to 2:1 (host:guest) complex formation. Addition of one molar equivalent of Na^+ or Ca^{2+}, however, again showed a single cv wave, but with a larger anodic shift which corresponded to 1:1 complex formation (Fig. 8). Addition of further cation did not change the cv, showing that a 1:1 complex was formed via a 2:1 (host:guest) complex which again confirms the results from uv–vis spectroscopy. It was also noticed that the 1:1 wave was sharper ($\Delta E_{1/2} \sim 70$ mV) than the 1:2 wave ($\Delta E_{1/2}$ ca. 110 mV) suggesting that the 2:1 wave may correspond to a mixture of 1:1 and 2:1 complexes which are exchanging rapidly on the cv time scale.

Addition of half an equivalent of Mg^{2+} showed two electrochemical waves with approximately the same

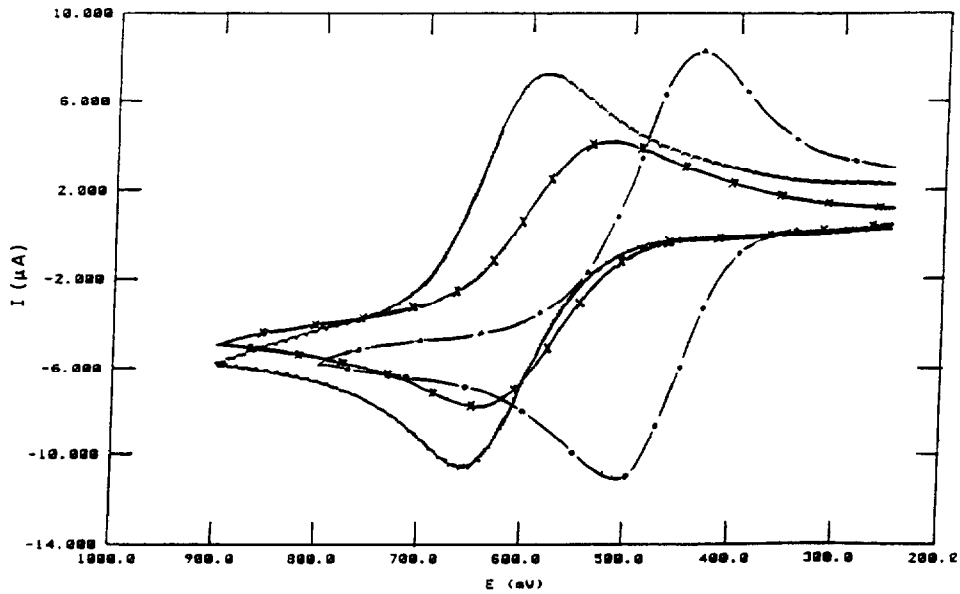

Fig. 8. Cyclic voltammograms for (5) complexing with Ca^{2+}: (– · – · –) free ligand; (– × – × –) 2(5) + Ca^{2+}; (———) (5) + Ca^{2+}.

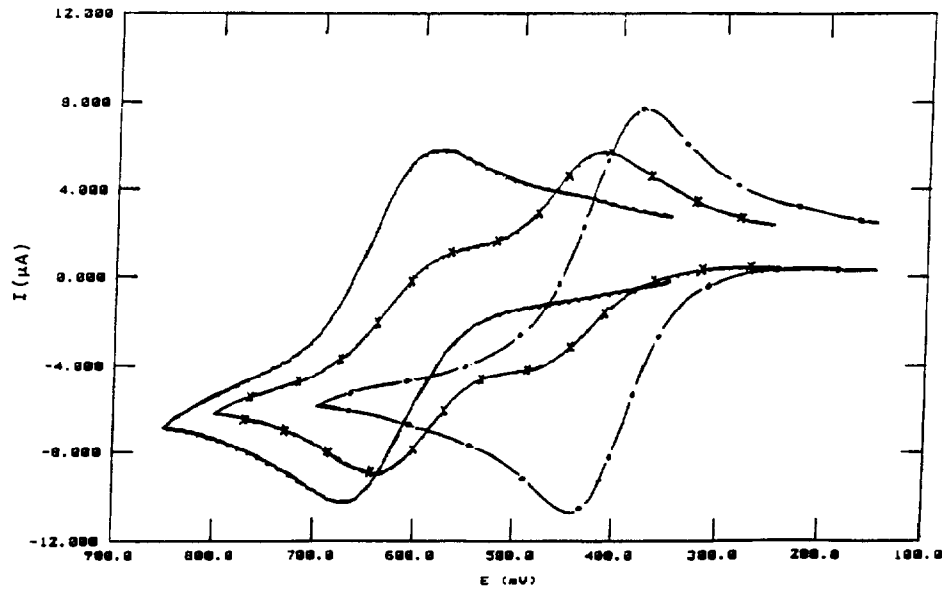

Fig. 9. Cyclic voltammograms for (5) complexing with Mg^{2+}: (– · – · –) free ligand, (– × – × –) 2(5) + Mg^{2+}; (———) (5) + Mg^{2+}.

intensity but different anodic shifts relative to that of the free ligand. The wave with the largest anodic shift probably corresponds to the 1 : 1 complex, and the one with the smaller shift to the 2 : 1 complex. Addition of a molar equivalent of Mg^{2+} led to the observation of a single cv wave with the same potential shift as the large anodic shift (Fig. 9). Thus it may be concluded that the 1 : 1 complex between (5) and Mg^{2+} was formed via the 2 : 1 complex, which again confirms the uv–vis data. Unlike the Na^{+} or Ca^{2+}, however, the equilibration between the 1 : 1 and 2 : 1 complexes must be slow on the cv time scale in order to observe two distinct cv waves.

Addition of half an equivalent of Tb^{3+} led to the observation of a large anodically shifted cv wave (the 2 : 1 complex) together with the hint of a second, less shifted cv wave assigned to a 3 : 1 complex (Fig. 10). This result was also consistent with the uv data which showed 3 : 1 complex formation but was unable to confirm a mixture of the two complexes. Addition of half an equivalent of Dy^{3+} or Yb^{3+} showed two cv waves with approximately the same intensity (Fig. 11)

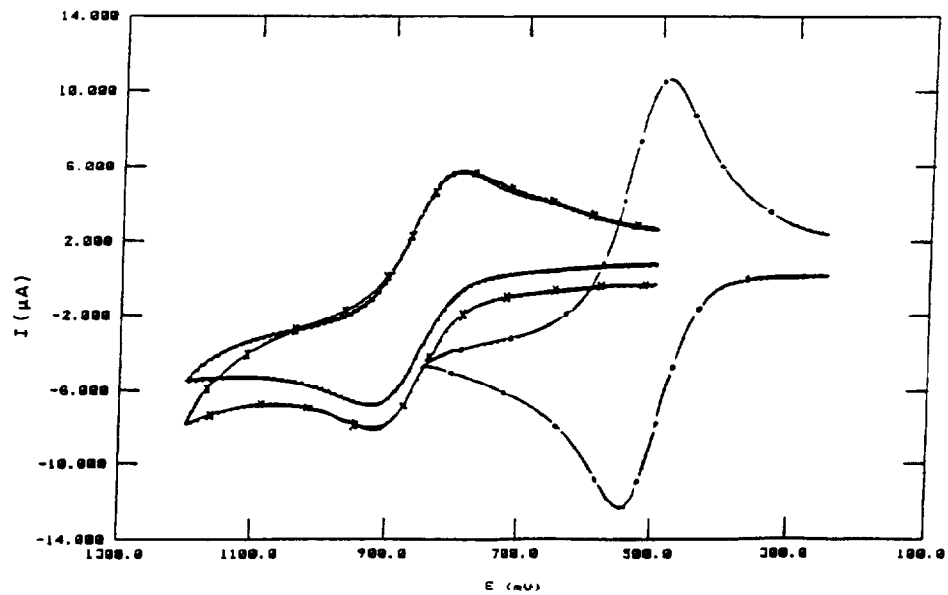

Fig. 10. Cyclic voltammograms for (5) complexing with Tb^{3+}: (– · – · –) free ligand; (– × – × –) 2(5) + Tb^{3+}; (———) (5) + Tb^{3+}.

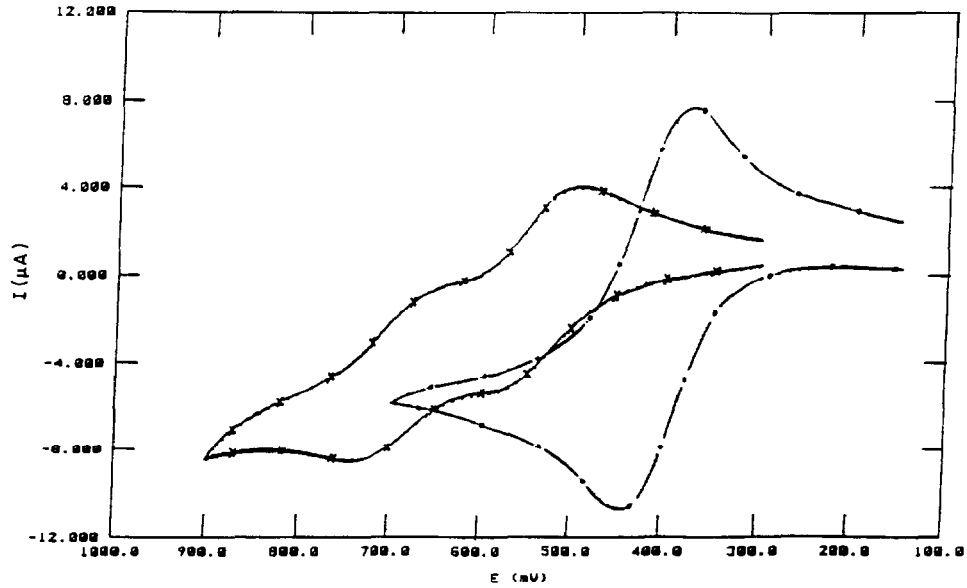

Fig. 11. Cyclic voltammograms for (5) complexed with Yb^{3+}: (– · – · –) free ligand; (– × – × –) 2(5) + Yb^{3+}.

which were assigned to a mixture of 2:1 and 3:1 complexes.

Finally, two cv waves were observed on addition of half an equivalent of Ag^+, which corresponded to a 1:1 complex plus the free ligand (Fig. 12). Addition of 1 molar equivalent of Ag^+ caused the oxidation wave of the free cryptand to be replaced by an intense oxidation wave of the complex. On the reduction sweep, however, a low intensity peak was observed for the 1:1 complex which was followed by a more intense reduction wave for the free cryptand (Fig. 12). Clearly the complex, once oxidised, dissociates owing to charge repulsion between the ferricinium unit and the guest cation.

The $\Delta E_{1/2}$ values for all the cryptates are shown in Table 3. The results were then analysed in terms of the stoichiometry of the cryptates and plots of $\Delta E_{1/2}$ vs. charge/radius (c/r) generated for each stoichiometry. Thus Fig. 13 shows a linear correlation for the 1:1 complexes of Na^+, Ca^{2+} and Mg^{2+} with (5); this indicates that the $\Delta E_{1/2}$ values are directly proportional to the polarisation of the carbonyl groups by the cations [12b]. In these cases, the effect on the redox potential of the ligand is transmitted *through bonds*, by coordination of the carbonyl groups with the cations. The 1:1 complex with Ag^+, however, showed a much larger value of $\Delta E_{1/2}$ (184 mV) than anticipated from its c/r value;

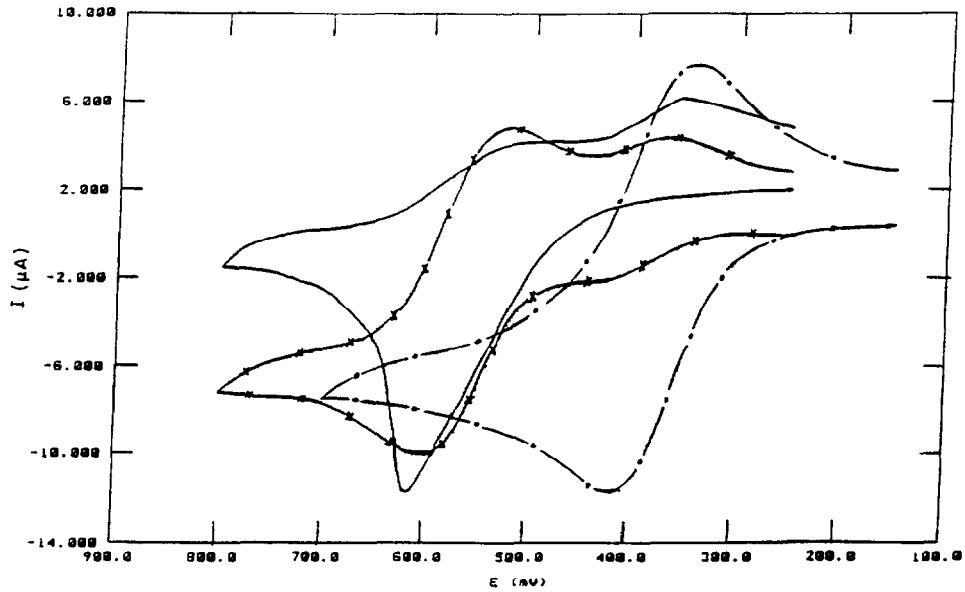

Fig. 12. Cyclic voltammograms for (5) complexed with Ag^+: (– · – · –) free ligand; (– × – × –) 2(5) + Ag^+; (———) (5) + Ag^+.

Table 3
Summary of cyclic voltammetry data for the complexation of (5) with a variety of mono-, di- and trivalent cations

Cation	r (Å)	c/r	$\Delta E_{1/2}$ (mV) [L/M]
Ag^+	1.26	0.79	184 [1/1]
Na^+	0.97	1.03	70 [1/1]
Mg^{2+}	0.66	3.03	223 [1/1]
Ca^{2+}	0.99	2.02	146 [1/1]
Sr^{2+}	1.12	1.78	136 [2/1]
Ba^{2+}	1.34	1.49	121 [2/1]
Y^{3+}	0.89	3.36	326 [2/1]
Eu^{3+}	0.95	3.16	302 [2/1]
Tb^{3+}	0.92	3.25	317 [2/1]
Dy^{3+}	0.91	3.30	291 [2/1]; 191 [3/1]
Yb^{3+}	0.86	3.49	236 [2/1]; 131 [3/1]

this suggests that Ag^+ may be encapsulated within the cage and, therefore, much closer to the ferrocenyl unit, as found by Gokel and co-workers [15] for complexes of ferrocene-containing ligands with Ag^+. This would also explain the apparently enhanced expulsion of Ag^+ from the cage on oxidation of the cryptate.

A plot of $\Delta E_{1/2}$ vs. c/r also gave a linear correlation for the 2:1 (L:M) complexes (Fig. 14) showing that complex formation between (5) and Ba^{2+}, Sr^{2+}, Eu^{3+}, Tb^{3+} and Y^{3+} also occurred via coordination with the carbonyl groups. This is probably the reason why uv irradiation of complexes of (5) with Eu^{3+}, Tb^{3+} and Yb^{3+} have so far failed to produce fluorescence in the expected visible region of the spectrum. Further studies in the area will therefore involve the reduced form of (5).

3. Experimental

^1H and ^{13}C NMR spectra were recorded on either Bruker AM360 or Bruker WX400 spectrometers using $CDCl_3$ and/or CD_3CN as solvents. Cyclic voltammograms were recorded using an EG & G Model 273 potentiostat with Model 270 software controlled by a

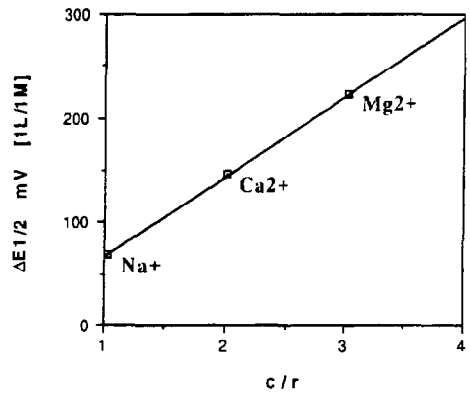

Fig. 13. Plot of $\Delta E_{1/2}$ vs. c/r for 1:1 complex of (5) with Na^+, Ca^{2+} and Mg^{2+}.

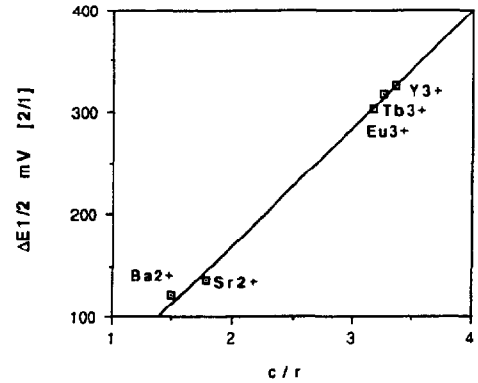

Fig. 14. Plot of $\Delta E_{1/2}$ vs. c/r for 1:1 complex of (5) with Sr^{2+}, Ba^{2+}, Eu^{3+}, Tb^{3+} and Y^{3+}.

Viglen computer connected to a Hewlett-Packard colour plotter for graphical output. The cyclic voltammetry experiments were conducted in dry propylene carbonate as solvent (ca. 1.5 mM in 5) with 0.1 M Bu_4NClO_4 (TBAP) as supporting electrolyte, a platinum wire in a solution of ferrocene (0.01 M) in propylene carbonate as the reference electrode and Pt wire as both working and counter electrodes. The scan rate was normally 100 mV s^{-1} with *IR* compensation applied during each scan.

Uv–vis spectra were recorded using a Hewlett-Packard Diode-Array 8452A spectrometer controlled by a Vectra QS/HS computer and fitted with a thermostatted cell compartment regulated to $+/-0.2$°C by a Grant thermostat waterbath. A solution of (5) at 10^{-3} M in $CHCl_3$–CH_3CN (50:50) was treated successively with 0.1 equivalents of each metal cation prepared as concentrated solutions of their triflates in CH_3CN and the absorbance of each solution recorded at constant wavelength (450 or 292 nm) until an excess of cation had been added. Plots of absorbance vs. cation concentration were then created to determine the stoichiometry of the complexes formed.

3.1. Synthesis of 1,1′(6,9-dioxa-3,12,23,26-tetraazatetracyclo[18.8.4.0^{17,25}.0^{20,24}]-hexacosa-1(22),14,16,18,20,23,25-heptaene-3,15-diyldicarbonyl)ferrocene (5)

A three-necked flask equipped with a mechanical stirrer was flushed with nitrogen and then charged with anhydrous toluene (250 ml). A solution of 1,1′-bis(chlorocarbonyl)ferrocene (0.45 g, 1.44 mmol) dissolved in anhydrous toluene (250 ml) was placed in a pressure-equalised dropping funnel. In a second similar dropping funnel was placed a solution containing the phenanthroline crown macrocycle (3, 0.50 g, 1.44 mmol) dissolved in anhydrous dichloromethane (200 ml) together with a solution of triethylamine (1.45 g, 14.4 mmol) in anhydrous toluene (50 ml). The two solutions were added dropwise, simultaneously over a period of 6 h to the

vigorously stirred toluene in the flask at room temperature. The mixture was stirred overnight when a fine precipitate of triethylamine hydrochloride was formed. The orange mixture was filtered, and the filtrate was evaporated to dryness to give an orange solid which was dissolved in dichloromethane (50 ml). The organic solution was washed with water (3 × 30 ml), then dried with Na_2SO_4 and evaporated to leave an orange solid. Flash chromatography on silica using dichloromethane (97%) and methanol (3%) removed polymers formed during the reaction. An orange band was collected, evaporated to dryness to give an orange solid which was chromatographed on neutral alumina with dichloromethane–methanol (99.75%:0.25%). An orange band was collected which, upon the removal of solvent under vacuum, yielded 200 mg of an orange powder (24%) m.p. greater than 250°C, RMM (FAB, 3NBA matrix = 591 for M + 1) and accurate FAB RMM, found for $(M + Na^+) = 613.1510$; calc. for $C_{32}H_{30}FeN_4NaO_4$, $M = 613.1514$. I.R. (KBr) ν (cm^{-1}) 1621 (C=O str. amide).

The ^1H and ^{13}C NMR data are shown in Tables 1(a) and (b).

3.2. Metal triflates

All the trifluoromethanesulphonate salts were prepared by treatment of the appropriate metal carbonate or oxide with the stoichiometric amount of triflic acid followed by evaporation of the residual water under high vaccuum (less than 0.01 mm Hg) at 130°C.

Acknowledgements

We are indebted to King's College, London for a Junior Research Scholarship (to TKUT) and to the Intercollegiate Research Services of the University of London for NMR spectra (KCL) and accurate FAB mass spectrometry data (Dr. K.J. Welham, School of Pharmacy).

References

[1] (a) P.D. Beer, *Adv. Inorg. Chem., 39* (1992) 79. (b) J.-M. Lehn, *Supramolecular Chemistry*, VCH, Weinheim, 1995, Chapter 8 (c) B. Dietrich, P. Viout, J.-M. Lehn, *Macrocyclic Chemistry*, VCH, Weinheim, 1993, Chapter 3.

[2] C.D. Hall, J.H.R. Tucker and S.Y.F. Chu, *J. Organomet. Chem., 448*, (1993) 175.

[3] A.P. Bell, P.J. Hammond and C.D. Hall, *J. Chem. Soc. Perkin Trans. 1*, (1983) 707.

[4] P.J. Hammond, P.D. Beer, C. Dudman, I.P. Danks and C.D. Hall, *J. Organomet. Chem., 306* (1986) 367.

[5] P.D. Beer, C.D. Bush and T.A. Hamor, *J. Organomet. Chem., 339* (1988) 133.

[6] M.C. Grossel, M.R. Goldspink, J.A. Jrıljac and S.C. Weston, *Organometallics, 10* (1991) 851.

[7] G.W. Gokel, in J.F. Stoddart (ed.), *Crown Ethers and Cryptands*, R.S.C. Monograph, 1991.

[8] A. Carroy and J.-M. Lehn, *J. Chem. Soc. Chem. Commun.*, (1986) 1232.

[9] T.E. Edmonds, in T.E. Edmonds (ed.), *Chemical Sensors*, Blackie, Glasgow and London, 1988, Chapter 8, p. 193.

[10] (a) J.-M. Lehn and G. Mathıs, *Angew Chem. Int. Ed. Engl., 19* (1990) 1304. (b) B. Alpha, J.-M. Lehn and G. Mathıs, *Angew Chem. Int. Ed. Engl., 26* (1987) 266.

[11] J.H.R Tucker, *Ph.D. Thesis*, University of London, 1993.

[12] (a) C.D. Hall, N.W. Sharpe, I.P. Danks and Y.P. Sang, *J. Chem. Soc. Chem. Commun.*, (1989) 149. (b) C.D. Hall and S.Y.F. Chu, *J. Organomet. Chem., 498* (1995) 221.

[13] (a) C.D. Hall, J.H.R. Tucker and N.W. Sharpe, *Organometallics, 10* (1991) 1727. (b) C.D. Hall, J.H.R. Tucker, S.Y.F. Chu, A.W. Parkins and S.C. Nyburg, *J. Chem. Soc. Chem. Commun.*, (1993) 1505.

[14] C.D. Hall, I.P. Danks, M.C. Lubienski and N.W. Sharpe, *J. Organomet. Chem., 384* (1990) 139.

[15] J.C. Medina, T.T. Goodnow, M.T. Rojas, J.L. Atwood, B.C. Lynn, A.E. Kaifer and G.W. Gokel, *J. Am. Chem. Soc., 114* (1992) 10583.